

Supplementary information

Mechanism of Cs Precursor Effect on Cs-Ag/Al₂O₃: Tuning Oxygen Activation for Ethylene Epoxidation

Liang Liu and Guangpeng Yang*

REZEL Catalysts Corp., Shanghai, 201313, China

*Corresponding author: gpyang2020@163.com

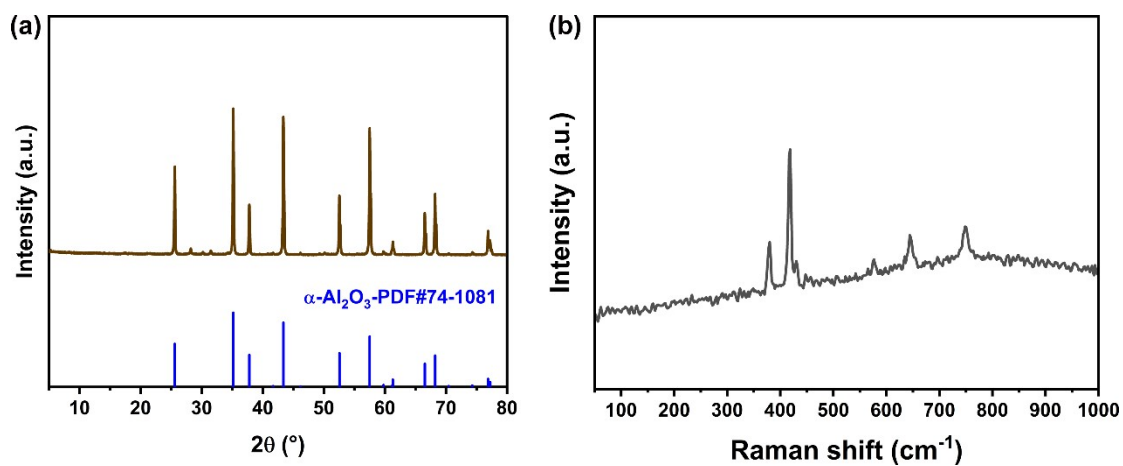


Fig. S1 (a) XRD pattern and (b) Raman spectra for pure Al_2O_3 sample.

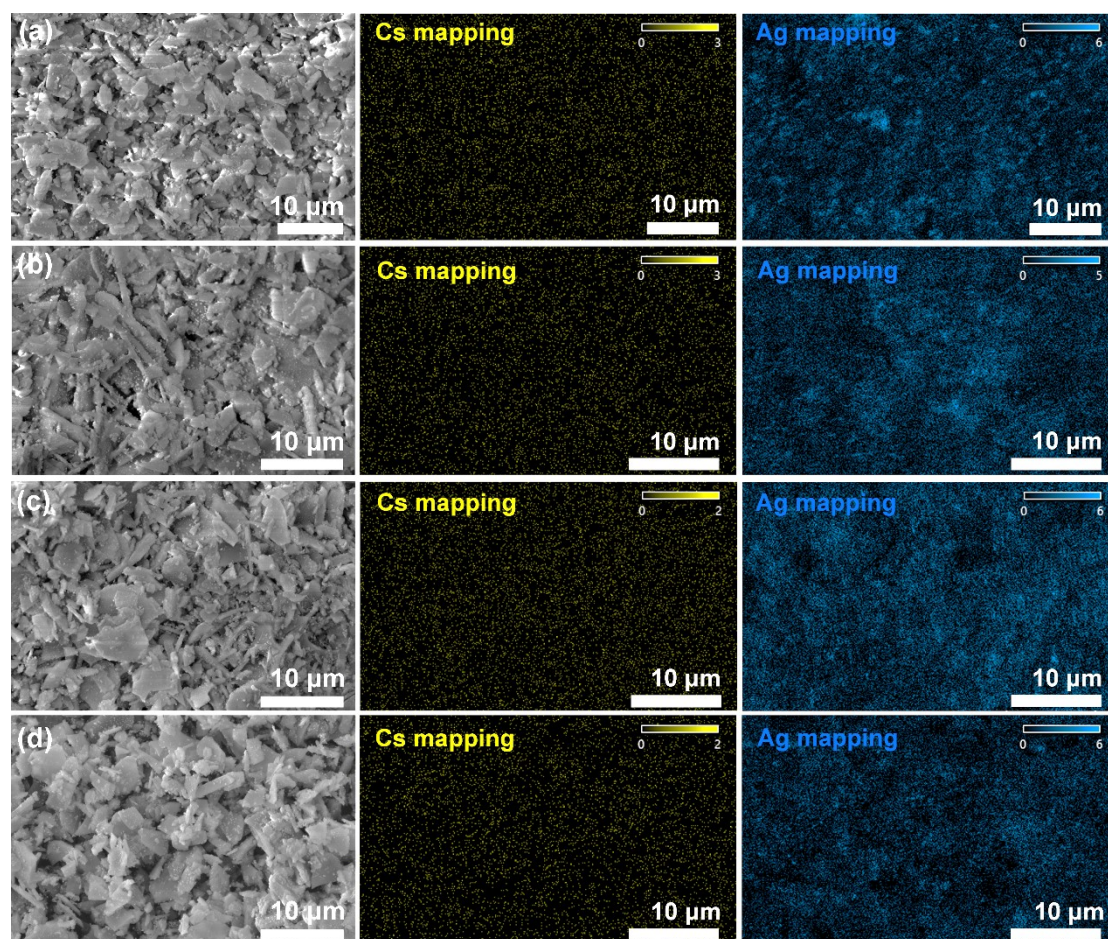


Fig. S2. SEM images with EDX maps of as-prepared $\text{Ag}/\text{Al}_2\text{O}_3$ and Cs-promoted $\text{Ag}/\text{Al}_2\text{O}_3$ (samples A, B and C).

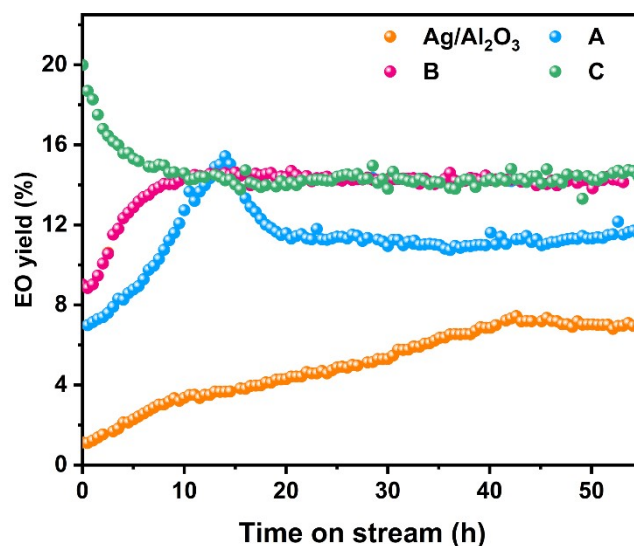


Fig. S3. EO yield during ethylene epoxidation along with the time on stream over Ag/Al₂O₃ and Cs-promoted Ag/Al₂O₃ (A, B and C) catalysts. Reaction conditions: T = 225 °C, P = 20 bar, C₂H₄:O₂:N₂ = 7.5 vol%/3.0 vol%/89.5 vol% and GHSV = 5100 h⁻¹.

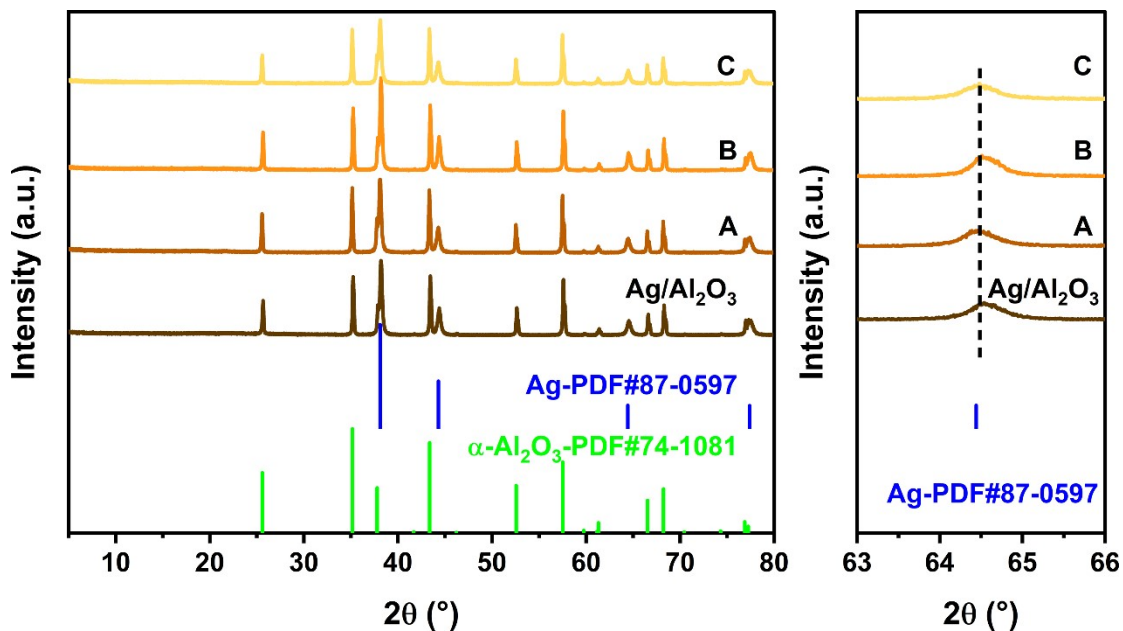


Fig. S4. XRD patterns of the used Al₂O₃, Ag/Al₂O₃ and Cs-promoted Ag/Al₂O₃ (A, B and C) samples.

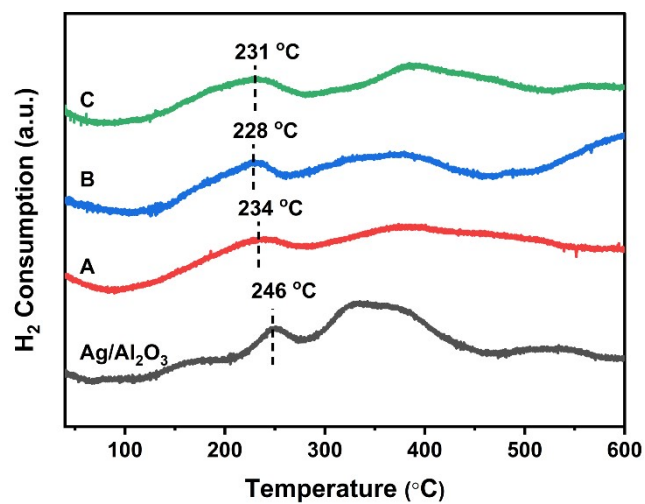


Fig. S5. H₂-TPR profiles of the used Ag/Al₂O₃ and Cs-promoted Ag/Al₂O₃ (A, B and C) samples.

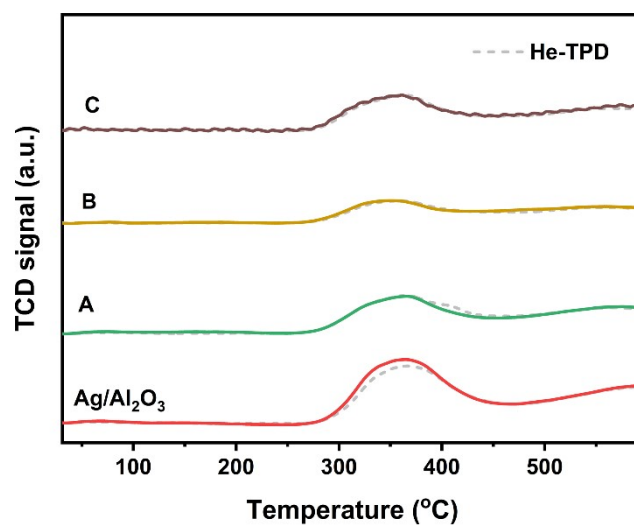


Fig. S6. C₂H₄-TPD and He-TPD (gray dot line) profiles of Ag/Al₂O₃ and Cs-promoted Ag/Al₂O₃ (samples A, B and C).

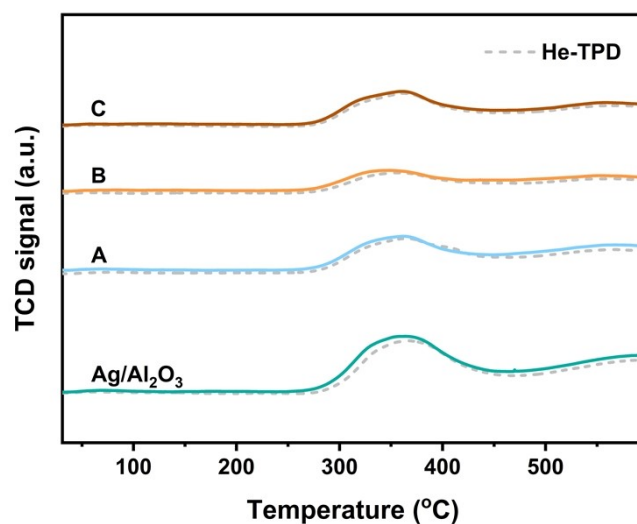


Fig. S7. CO₂-TPD and He-TPD (gray dot line) profiles of Ag/Al₂O₃ and Cs-promoted Ag/Al₂O₃ (samples A, B and C).

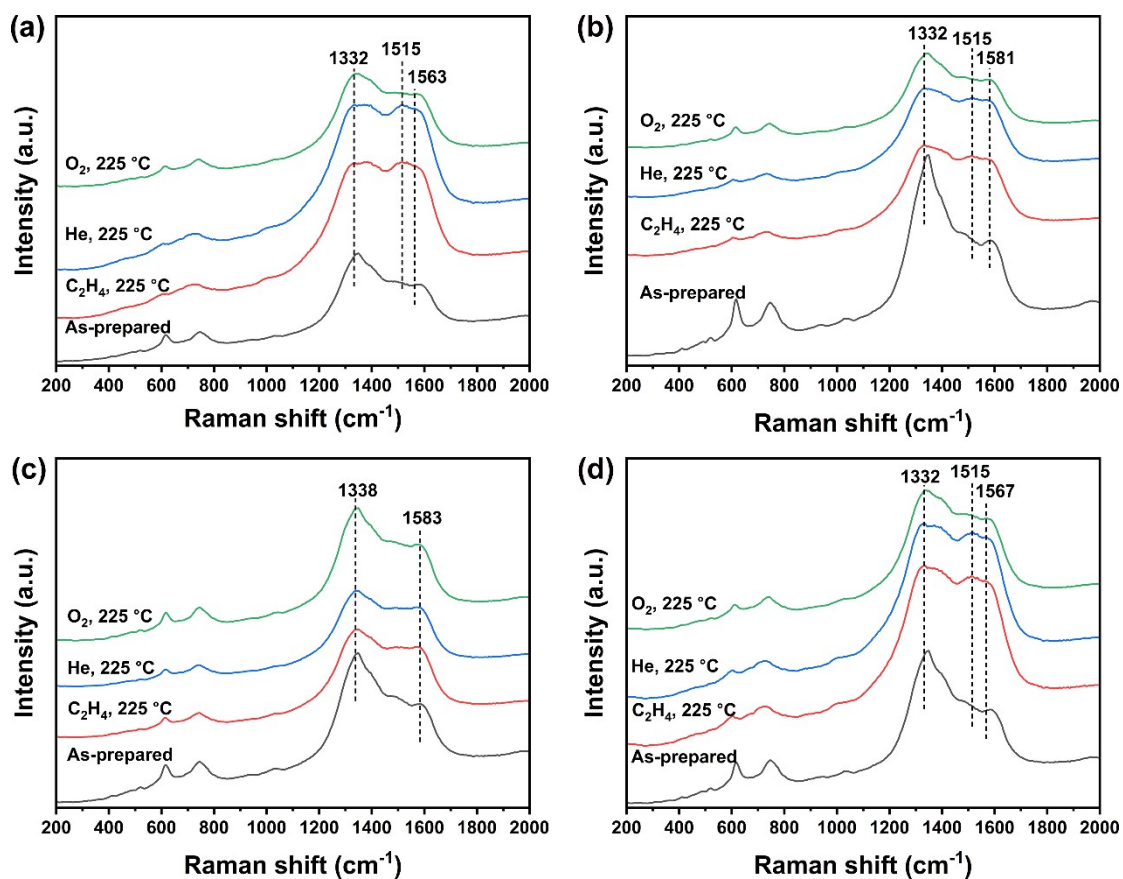


Fig. S8. Raman spectra during ethylene adsorption over (a) Ag/Al₂O₃, (b) sample A, (c) sample B, and (d) sample C.

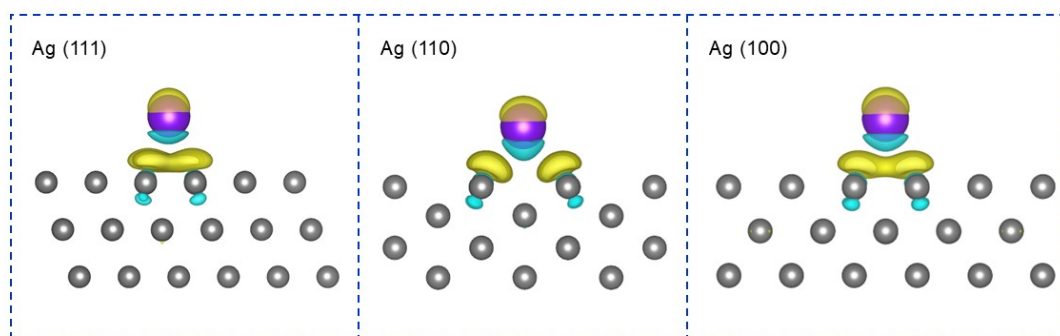


Fig. S9. Isosurfaces (isovalue = 0.001) of the charge density difference of the Cs-modified Ag (111), Ag (110) and Ag (100) surfaces using density functional theory (DFT) calculations. Gray and purple spheres represent Ag atoms and Cs atoms, respectively. Yellow and blue isosurfaces correspond to charge accumulation and charge depletion regions, respectively.

Table S1. Physical properties of the as-prepared Ag/Al₂O₃ and A, B, C catalysts.

| Sample | Ag (wt%) ^a | Cs (wt%) ^a | As-prepared | | Used | |
|-----------------------------------|--------------------------|--------------------------|--|--|--|--|
| | | | Ag d _{XRD} (nm) ^b | Ag d _{SEM} (nm) ^c | Ag d _{XRD} (nm) ^b | Ag d _{SEM} (nm) ^c |
| Ag/Al ₂ O ₃ | 13.12 | - | 38.9 | 159 ± 1 | 44.8 | 165 ± 4 |
| A | 12.97 | 0.04 | 35.6 | 88 ± 1 | 41.2 | 128 ± 2 |
| B | 13.24 | 0.04 | 33.4 | 80 ± 1 | 45.1 | 132 ± 3 |
| C | 12.93 | 0.04 | 33.2 | 93 ± 1 | 40.7 | 125 ± 3 |

^a Determined by ICP-OES.

^b The Ag particle size was estimated based on the XRD line broadening of the Ag (220) diffraction peak.

^c The Ag particle size was estimated from SEM images by counting 250-300 silver particles across at least three different regions, assuming a spherical morphology.

Table S2. O₂-TPD data for Ag/Al₂O₃ and A, B, C samples.

| Sample | I ₁ /I ₂ ratio | O ₂ desorption (μmol g _{cat} ⁻¹) ^a |
|-----------------------------------|--------------------------------------|--|
| Ag/Al ₂ O ₃ | 0.99 | 13.5 |
| A | 0.87 | 21.7 |
| B | 0.93 | 24.6 |
| C | 0.92 | 21.5 |

^a Determined by the integrated area of the reduction peak from 150 to 350 °C.

Computational Details

All DFT calculations were carried out using the CP2K Code.¹ Perdew-Burke-Ernzerhof (PBE) within the generalized gradient approximation (GGA) was applied to treat exchange correlation functions. The Geodecker–Teter–Hutter (GTH) pseudopotentials were implemented to describe core electrons, with the hybrid Gaussian and plane waves framework (GPW).² The valence molecular orbitals were expanded using molecularly optimized (MOLOPT) Gaussian-type basis sets.³ A Monkhorst–Pack $3 \times 3 \times 1$ K-point sampling was used, with a 500 Ry cutoff energy. Three kinds of Cs-doped metallic silver facets ((111), (110), (100)) are considered.⁴ These structures were optimized within periodic boundary conditions using three layers of a 4×4 unit cell. Isosurfaces of the charge density difference of the Cs-modified Ag (111), Ag (110) and Ag (100) surfaces were shown in Fig. S9.

References

1. J. VandeVondele, M. Krack, F. Mohamed, M. Parrinello, T. Chassaing, J. Hutter, Quickstep: Fast and accurate density functional calculations using a mixed Gaussian and plane waves approach, *Computer Physics Communications*, 2005, **167**, 103-128.
2. S. Goedecker, M. Teter, J. Hutter, Separable dual-space Gaussian pseudopotentials, *Physical Review B*, 1996, **54**, 1703-1710.
3. J. VandeVondele, J. Hutter, Gaussian basis sets for accurate calculations on molecular systems in gas and condensed phases, *The Journal of Chemical Physics*, 2007, **127**, 114105.
4. T. Pu, A. Setiawan, A. C. Foucher, M. Guo, J. M. Jehng, M. Zhu, M. E. Ford, E. A. Stach, S. Rangarajan, I. E. Wachs, Revealing the Nature of Active Oxygen Species and Reaction Mechanism of Ethylene Epoxidation by Supported Ag/ α -Al₂O₃ Catalysts, *ACS Catalysis*, 2024, **14**, 406-417.